In vitro and ex vivo assessment of microporous Faujasite zeolite (NaX-FAU) as a carrier for the oral delivery of danazol

Accepted Manuscript

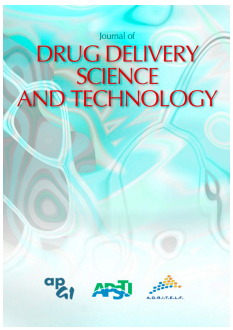

In vitro and *ex vivo* assessment of microporous Faujasite zeolite (NaX-FAU) as a carrier for the oral delivery of danazol

Eleni Kontogiannidou, Christina Karavasili, Maria G. Kouskoura, Maria Filippousi, Gustaaf Van Tendeloo, Ioannis I. Andreadis, Georgios K. Eleftheriadis, Ioanna Kontopoulou, Catherine K. Markopoulou, Nikolaos Bouropoulos, Dimitrios G. Fatouros

PII: S1773-2247(18)31329-7

DOI: https://doi.org/10.1016/j.jddst.2019.02.036

Reference: JDDST 963

To appear in: *Journal of Drug Delivery Science and Technology*

Received Date: 5 December 2018

Revised Date: 23 February 2019

Accepted Date: 27 February 2019

Please cite this article as: E. Kontogiannidou, C. Karavasili, M.G. Kouskoura, M. Filippousi, G. Van Tendeloo, I.I. Andreadis, G.K. Eleftheriadis, I. Kontopoulou, C.K. Markopoulou, N. Bouropoulos, D.G. Fatouros, *In vitro* and *ex vivo* assessment of microporous Faujasite zeolite (NaX-FAU) as a carrier for the oral delivery of danazol, *Journal of Drug Delivery Science and Technology* (2019), doi: https://doi.org/10.1016/j.jddst.2019.02.036.

Graphical Abstract

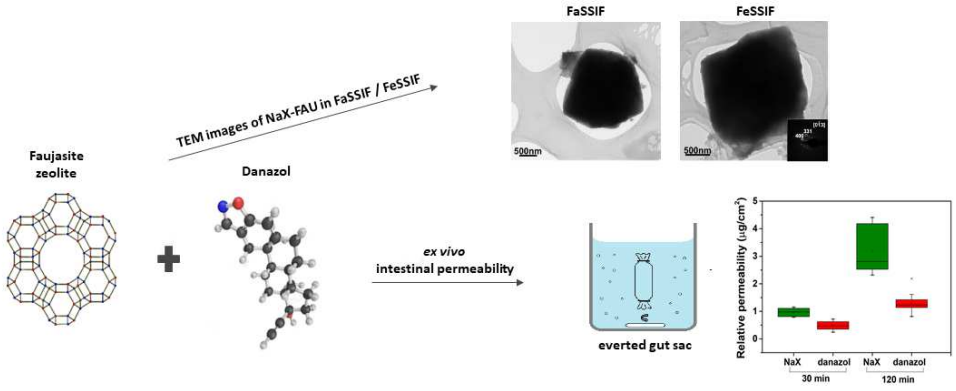

In vitro and *ex vivo* assessment of microporous Faujasite zeolite (NaX-FAU) as a carrier for the oral delivery of danazol

Eleni Kontogiannidou[1], Christina Karavasili[1], Maria G. Kouskoura[2], Maria Filippousi[3], Gustaaf Van Tendeloo[3], Ioannis I. Andreadis[1], Georgios K. Eleftheriadis[1], Ioanna Kontopoulou[4], Catherine K. Markopoulou[2], Nikolaos Bouropoulos[4,5], Dimitrios G. Fatouros[1,*]

[1]Laboratory of Pharmaceutical Technology, Department of Pharmaceutical Sciences, Aristotle University of Thessaloniki, GR-54124 Thessaloniki, Greece

[2]Laboratory of Pharmaceutical Analysis, Department of Pharmaceutical Sciences, Aristotle University of Thessaloniki, GR-54124 Thessaloniki, Greece

[3]EMAT, University of Antwerp, Groenenborgerlaan 171, B-2020 Antwerp, Belgium

[4]Department of Materials Science, University of Patras, 26504 Rio, Patras, Greece

[5]Foundation for Research and Technology Hellas, Institute of Chemical Engineering and High Temperature Chemical Processes, Patras, Greece

[*]Corresponding author: Dr Dimitrios G. Fatouros

e-mail: dfatouro@pharm.auth.gr

Tel: +30 2310 997653

Fax: +30 2310 997652

Abstract

Microporous zeolite NaX-FAU has been systemically evaluated for the oral delivery of the poorly water-soluble compound danazol. For this purpose, danazol-loaded zeolitic particles were prepared by the incipient wetness method and were characterized by means of N_2 physisorption, X-ray diffraction (XRD), differential scanning calorimetry (DSC), thermogravimetric analysis (TGA) and high-resolution transmission electron microscopy (HRTEM). The zeolitic formulation shows a high drug payload and drug stability over a period of six months under accelerated storage conditions. The dissolution profile of danazol-loaded zeolitic particles was assessed in simulated gastric fluid (SGF) pH 1.2; fasted state simulated intestinal fluids (FaSSIF) and fed state simulated intestinal fluid (FeSSIF) showing a gradual and increasing drug dissolution in the different media. *Ex vivo* studies using the everted gut sac model show an increased drug transport across rat intestinal epithelium when loaded in the zeolitic particles. Our results suggest that microporous Faujasite zeolite (NaX-FAU) could be used as a drug delivery system to facilitate the oral delivery of poorly water soluble compounds.

Keywords: oral delivery, NaX-FAU zeolite, danazol, simulated intestinal fluids, intestinal absorption

1. Introduction

Oral drug absorption encounters multiple restraints commonly originating from the physicochemical properties of the active compounds. Since the majority of active compounds suffer from poor aqueous solubility, dissolution throughout the gastrointestinal tract is insufficient, resulting in poor drug permeability and low bioavailability after oral administration [1].

The use of porous inorganic materials has emerged as a formulation strategy to increase the solubility of sparingly soluble compounds [2-3]. Drug encapsulation into the porous matrices facilitates conversion of the crystalline form of the drug into its amorphous state of higher free energy, which in turn can increase its solubility [4-6].

Several inorganic materials have being explored as drug carriers opening new possibilities for biomedical applications [7]. Zeolites are among those materials that have enticed considerable attention in drug delivery, due to their innate unique properties [8-26]. Furthermore, it is possible that zeolites provide protection for drugs that are easily decomposed due to humidity, such as degradation [26]. Zeolites are microporous aluminosilicate materials based on an infinitely extending three-dimensional framework of SiO_4 and AlO_4 tetrahedra linked to each other by sharing oxygens that results in a uniform network of channels and pores (pore size < 2 nm) [27]. On the contrary, ordered mesoporous materials are amorphous silicate materials with highly ordered hexagonal arrangements of pores (channels or cages) with narrow size distributions in the mesoscale range (2-50 nm) [28].

The biological properties (non-toxicity and good biocompatibility) and stability in biological environments have rendered zeolites appropriate for medical use, mainly as drug delivery systems [29]. So far, zeolites have been successfully used as detoxicants and decontaminants, when added in animal nutrition, as well as antibacterial and

antidiarrheal agents. Although zeolites have been used in veterinary medicine and zootechnology, *in vivo* studies using zeolitic particles are relatively scarce [30]. In a study, the supplementation of the normal diet with two clinoptilolite dietary supplements (Megamin and Lycopenomin) in immunocompromised patients was accompanied with absence of any side effects and significant reduction of lymphocytes

CD56+ and significant increase of CD4+, CD19+ and CD3+ lymphocytes [31]. Potgieter and co-researchers investigated the effect of Absorbatox™ 2.4 D clinoptilolite as a gastroprotective agent in patients with endoscopically negative gastroesophageal reflux disease (ENGORD) and nonsteroidal anti-inflammatory drug induced gastritis [32]. A significant reduction in heartburn, discomfort and pain was reported in the patients receiving the clinoptilolite treatment [32].

In view of the promise of zeolites as carriers for oral drug administration, we loaded NaX-FAU zeolite with danazol, a BCS class II non-ionizable compound with low aqueous solubility (0.4-0.6 μg/mL) [33 -34] and limited bioavailability after oral administration, and further characterized the formulation by means of various physicochemical techniques. Faujasite is a mineral group in the zeolite family of silicate minerals. Its structure consists of truncated octahedra interconnected through double six-membered rings. The pores are defined by a 12-membered oxygen ring with an aperture of 7.4 Å and their interconnection leads to the formation of the main cavities of the zeolite. The silica to alumina ratio is the determinant factor of the zeolite type (X or Y), with high aluminum contents resulting in high exchange capacities that constitute zeolites useful in ion-exchange and adsorption applications, as well as molecular sieves in drug delivery applications, enabling control over drug loading and release kinetics based on the zeolite framework [27]. *In vitro* release

studies of the loaded particles were performed in simulated gastric and intestinal fluids, whereas their *ex vivo* performance was assessed using the everted sac-model. Finally, these studies were complemented by stability tests of the formulation under accelerated storage conditions.

2. Materials and methods

Zeolite NaX-FAU (SiO_2/Al_2O_3: 1.2) was obtained from Sigma-Aldrich (St. Louis, MO, USA). NaX-FAU belongs to the cubic system containing supercages with ~ 13 Å that communicate through ~7.35 Å windows [27]. Danazol was purchased from Alfa-Aesar (Germany). SIF powder for preparing FaSSIF and FeSSIF was purchased from Biorelevant.com. All chemicals and solvents were of analytical grade. Distilled water was used in all experimental procedures.

2.1 Preparation of release media

Phosphate buffered saline (PBS) pH 7.4, was prepared by dissolving NaCl (8.0 g), KCl (0.20 g), Na_2HPO_4 (1.44 g) and KH_2PO_4 (0.24 g) in 1 L of distilled water with 2% w/v sodium lauryl sulfate (SLS). Simulated gastric fluid (SGF) pH 1.2 was prepared by mixing 2 g of NaCl, 70 mL of 1M HCl and 930 mL of distilled water in the presence of 2 % w/v sodium lauryl sulfate (SLS). Fasted state simulated intestinal fluid (FaSSIF) [BS (sodium taurocholate) 3 mM; phospholipid (lecithin) 0.75 mM; Sodium dihydrogen phosphate (mM) 28.65; hydrochloric acid, sodium chloride 105.85 mM; Osmolarity (mOsmol/kg) ~270; Buffer capacity (mEq/pH/l) ~12; pH 6.5] and fed state simulated intestinal fluid (FeSSIF) [BS (sodium taurocholate) 15.75 mM; phospholipid (lecithin) 3.75 mM; acetic acid 144.05, hydrochloric acid, sodium chloride 203.18 mM; Osmolarity (mOsmol/kg) ~670; Buffer capacity

(mEq/pH/l) ~72; pH 5.0] were prepared with simulated intestinal fluid (SIF) powder, according to the manufacturer's instructions (Biorelevant.com Ltd, Croydon, Surrey, UK). FaSSIF and FeSSIF fluids were used to reflect the physiological conditions in human gastrointestinal tract [35]. Krebs Ringer solution (pH 7.4) was used in the *ex vivo* studies and was prepared with 0.67 % w/v sodium chloride, 0.034 % w/v potassium chloride, 0.059 % w/v magnesium sulphate, 0.011 % w/v calcium chloride, 0.234 % w/v sodium dihydrogen phosphate and 0.18 % w/v glucose in distilled water. In all cases, media were used within 24 h after preparation.

2.2 Preparation of the danazol loaded NaX-FAU formulations

The incipient wetness impregnation was the method adopted to achieve danazol loading within the NaX-FAU zeolite. Oven-drying of the NaX-FAU zeolite was performed at 120 ^{o}C prior to drug loading for 24 h to remove the adsorbed moisture. A methylene chloride solution of danazol was added under vigorous stirring in the dried zeolite powder at a 1:2 weight ratio. Samples were then dried at 40 ^{o}C for at least 48 h to remove traces of the organic solvent and were further stored in a desiccator.

2.3 Determination of drug loading efficiency

2.3.1 Extraction method

Danazol content in the NaX-FAU formulations was quantified using the extraction method described below. One milligram of each sample was dispersed in 10 mL of PBS pH 7.4 (2 % w/v SLS) and was magnetically stirred for 24 h at 37 ^{o}C. The dispersions were then centrifuged at 4500 rpm for 15 min, the supernatants were filtered through a PTFE filter with 0.45 μm pore size and drug content was quantified

with UV spectroscopy (UV mini-1240, SHIMADZU) at 287 nm. Drug content was calculated according to following equation:

$$\text{Drug content } (\%) = \frac{weight\ of\ danazol\ in\ the\ particles}{weight\ of\ particles} \text{ x } 100 \quad (1)$$

2.3.2 Thermogravimetric analysis (TGA)

Danazol content in the NaX-FAU formulation was additionally quantified with thermogravimetric analysis using a TGA Q500 apparatus (TA instruments Ltd.). Samples (danazol, NaX-FAU, danazol-NaX-FAU) were analyzed in air atmosphere at a heating rate of 10 °C/min and in the temperature range from 40 °C to 800 °C. Thermal equilibration of the samples was performed at 40 °C prior to analysis to remove the excess moisture.

2.4 Physicochemical characterization

2.4.1 ζ-potential measurements

The surface charge of the empty and danazol loaded NaX-FAU formulations was determined using a Zetasizer Nanoseries, Nano-ZS analyzer (Malvern, UK) at 25 ^{o}C. The samples were dispersed in distilled water at a total solid load of 1 % wt. and briefly sonicated to enable homogenous dispersion in the medium prior to measurements.

2.4.2 Differential scanning calorimetry (DSC)

The thermal properties of the samples were characterized with differential scanning calorimetry (DSC) using a DSC 204 F1 Phoenix apparatus (NETZSCH). Samples were sealed in perforated aluminum pans and scanned at a heating rate of 10 ^{o}C/min under a nitrogen purge of 70 mL/min and at the temperature range from 30 ^{o}C to 250 ^{o}C.

126

127 *2.4.2 X-ray diffraction (XRD)*

128 The solid-state properties of danazol in the NaX-FAU formulation were evaluated
129 with
130 XRD analysis. Diffractograms were recorded on a Bruker D8-Advance diffractometer
131 (Bruker AXS GmbH, Karlsruhe, Germany) using Cu Kα radiation (λ = 1.5421 Å)
132 operated at a voltage and current of 40 kV and 40 mA, respectively. Samples were
133 scanned over the 2θ range of 3-50˚ at a rate of 0.35 s/step with a step size of 0.02^{o}.

134

135 *2.4.4 Physisorption studies*

136 The textural properties of the samples were investigated with a Quantachrome Nova
137 2200E Surface Area and Pore Size Analyzer (Quantachrome Instruments, Boynton
138 Beach, Florida, USA) using the Brunauer-Emmett-Teller (BET) method. Prior to
139 analysis, samples were degassed at 50 ^{o}C to ensure minimum water vapor in the
140 samples. N_2 Adsorption/desorption isotherms were recorded at -196 ^{o}C. The specific
141 surface area was calculated using experimental points at a relative pressure of P/P_o =
142 0.02 - 0.04. The micropore area and external surface area were assessed using the t-
143 plot method in the relative pressure range from 0.2 to 0.4. The N_2 isotherms were
144 analyzed using the Saito-Foley (SF) approximation for cylindrical pore geometry to
145 obtain pore size distributions. The total pore volume was calculated by measuring the
146 amount of N_2 adsorbed at 0.995 P/P_o.

147

148 *2.4.5 Visualization of zeolitic particles using high resolution transmission electron*
149 *microscopy*

Samples suitable for transmission electron microscopy measurements were prepared by drop casting an ethanolic solution containing pristine NaX-FAU particles on holey carbon-coated copper grids using a Tecnai G2 electron microscope operated at 200 kV.

2.5 Stressing tests

Accelerated stability studies were conducted to assess changes in the crystalline state of danazol in the NaX-FAU formulations. Samples were stored at 40 ± 2 ^{o}C and 75 ± 5 % RH in stability chambers for 6 months and then subjected to DSC and XRD analysis.

2.5.1 Stability studies in simulated intestinal fluids

The stability of NaX-FAU zeolite was assessed in simulated intestinal media under fasted and fed state conditions. NaX-FAU (2 mg) was dispersed in FaSSIF and FeSSIF media for 2 h at 37 ^{o}C. Samples suitable for transmission electron microscopy were prepared by drop casting the dispersion on holey carbon-coated copper grids. Low and high magnification TEM images and selected area electron diffraction (SAED) patterns were acquired using a Tecnai G2 electron microscope operated at 200 kV.

2.6 In vitro drug release in simulated gastric fluid and simulated intestinal fluids

In vitro drug release studies were performed in 20 mL of medium (SGF in the presence of 2 % w/v SLS, FaSSIF and FeSSIF) in a shaking water bath at 37 °C. The drug loaded zeolitic formulation (equivalent to 200 μg of danazol) was dispersed in each medium and samples (0.1 mL) were withdrawn and replaced with an equal volume of preheated medium to maintain a constant release volume. All experiments were carried out in quadruplicates. The samples were further analyzed by HPLC as described in section 2.8.

2.7 Determination of ex vivo intestinal permeability

Intestinal permeability studies were conducted using the everted sac method to assess the effect of zeolite on intestinal drug absorption [35], [36]. Wistar rats fasted overnight with access to water ad libitum were euthanized and the jejenum was excised and rinsed with ice-cold Krebs-Ringer solution [37]. Subsequently, the tissue was gently everted using a glass rod and was cut in segments (5 cm in length), obviating intestinal regions containing Peyer's patches. Each segment was tied at one end with a cotton thread, filled with 0.5 mL Krebs-Ringer solution and then tied at the other end. The sacs were placed in 20 mL capped glass vials containing oxygenated Krebs-Ringer solution and the zeolitic formulation (corresponding to 1.5 mg of danazol) in a shaking water bath at 37 ^{o}C. A dispersion of pure danazol (1.5 mg) served as the control. The sacs were removed at predetermined time points, rinsed with Krebs-Ringer solution and blotted dry. After measuring their dimensions (width, length) they were cut open and the serosal fluid was collected and centrifuged at 10,000 g for 15 min. Danazol was quantified in the supernatants with HPLC analysis ($n \geq 4$). Relative permeability was calculated as the amount (μg) of transported danazol per intestinal mucosal surface area (cm^2) according to Equation 2 [38 -39] :

$$\text{Relative permeability} = \frac{(\text{Danazol concentration})_{serosal\ fluid} \times (\text{Volume})_{serosal\ fluid}}{(\text{Surface area})_{mucosal}} \quad (2)$$

2.8 HPLC analysis

Prior to HPLC analysis, samples were centrifuged at 10,000 g for 10 min and the supernatants were filtered through a PTFE filter with 0.45 μm pore size. The drug content was quantified using a High-Performance Liquid Chromatography instrument (Shimadzu) equipped with two LC LC-20AD pumps, a SIL-10AD auto-sampler and a UV-diode array detector. The experimental conditions were maintained at 25 ˚C with the use of a Shimadzu column oven. The stationary phase was an octadecyl (C18) column (dimensions 150x4.6 mm and 5 μm particle size). The mobile phase consisted of 50 % MeON:H_2O. The flow rate of the mobile phase was adjusted to 0.8 mL/min and the injection volume was 90 μL. UV detection was performed at 287 nm. The chromatographic peaks were recorded and elaborated with LC Solution software. All solvents were filtered through a 0.45-mm nylon membrane and degassed prior to use. The calibration curves for danazol were linear ($r^2 > 0.999$) in the range of 0.1 - 50 μg/mL for all tested media.

2.9 Statistical analysis

All data are presented as mean values and standard deviation (± S.D.). Univariate statistical analysis was performed using t-test algorithm (tail 2, type 3) in Microsoft Excel. $P < 0.05$ was considered statistically significant.

3. Results and Discussion

The calculated danazol loading of the zeolitic particles as determined by UV and thermogravimetric analysis (Table 1) was in close agreement with the theoretical drug

payload (was 33.3 % w/w). The TGA curves of the NaX-FAU zeolite and danazol are represented by a one stage weight loss (Figure 1A) attributed to the desorption of physically adsorbed water and the thermal decomposition of the drug, respectively [24]. The TGA curve of the drug-loaded formulation was characterized by a three-stage weight loss. The second and third weight losses correspond to the thermal decomposition of danazol, located on the external surface area and within the pore structure of the zeolites, respectively. Consistent with the presence of adsorbed danazol onto the surface of zeolitic particles, the ζ-potential of drug-loaded particles (-32.7 ± 1.4 mV) was remarkably higher than that of the pristine zeolitic particles (-55.1 ± 2.4 mV) (Table 1).

The drug crystallinity after the incipient wetness method was evaluated by thermal (Figure 1B) and XRD (Figure 1C) analysis. In the zeolite thermograms, a weak and broad endothermic peak was observed from 60 ^{o}C to 160 ^{o}C attributed to the evaporation of physically adsorbed water. Danazol demonstrated a characteristic melting peak at 224 ^{o}C [41]. After its incorporation into the microporous zeolite, the drug's melting enthalpy decreased, due to the partial amorphization of danazol. The diffraction pattern of pure danazol demonstrates that the drug is highly crystalline and possesses multiple diffraction peaks in the 10°-30° 2θ range, in accordance with the literature [41]. The diffraction data of NaX-FAU are in perfect agreement with the patterns of the respective reference materials of similar framework topologies [42]. The crystallinity of NaX-FAU is retained after drug loading and the decrease in peak intensity at 6.2° can be possibly attributed to the masking effect of danazol deposited onto the external surface of the zeolite. However, the x-ray diffractogram of NaX-FAU loaded sample showed the presence of crystalline drug at 13^{o} and 17^{o} degrees,

248 further corroborating the results obtained from DSC for the partial amorphization of
249 the API.

250 The textural properties of the zeolitic particles prior- and post-drug loading were
251 evaluated by nitrogen sorption measurements and results are summarized in Table 2.
252 The N_2 sorption isotherms of both samples resemble Type I isotherms [4], indicating
253 the presence of micropore frameworks (Figure 2A). Nitrogen sorption isotherms
254 retain their characteristic shape post-incipient wetness method, indicating the
255 maintenance of the zeolite microporosity. The pore size distribution of plain NaX-
256 FAU and danazol-loaded zeolitic particles is illustrated in Figure 2B. A significant
257 decrease in the micropore area, external surface area and total pore volume of the
258 NaX-FAU particles (Table 2) was observed after danazol loading, denoting the
259 presence of the drug at the carrier with drug deposition occurring both on the external
260 surface area and within the micropores of the zeolitic carrier.

261 Low and high magnification TEM images of pure NaX-FAU zeolitic particles are
262 illustrated at Figure 3. A low magnification TEM image of the pristine NaX-FAU
263 particles and the corresponding SAED pattern of the biggest particle oriented along a
264 <110> zone axis is given as an inset in Figure 3A. Figure 3B represents an HRTEM
265 image of a thin edge of the same particle, with the corresponding fast Fourier
266 transform (FFT) given as an inset.

267 The thermodynamic instability of amorphous drug compounds is a significant
268 challenge especially for amorphous drug compounds during storage, since they tend
269 to convert back to the stable crystalline state over time. The state of danazol in the
270 zeolitic formulation was evaluated by DSC and XRD analysis. As shown in Figure 4
271 (A & B), the sample exhibits good physicochemical stability under accelerated
272 storage conditions of temperature and humidity (40 ± 2^{o}C and 75 ± 5% RH) for 6

months, without any changes been recorded in the thermograms and diffractograms over time.

Low and high magnification TEM images of the empty and drug loaded zeolitic particles were recorded in FaSSIF (Figures 5A and B) and FeSSIF (Figures 5C-F) media. The zeolitic carrier retained its structural integrity, since no alteration on the morphology or the structure of the zeolitic particles could be identified upon exposure to both media.

The dissolution of danazol-loaded NaX-FAU zeolitic particles and pure crystalline API were assessed in SGF pH 1.2 (in the presence of 2 % SLS), FaSSIF pH 6.5 and FeSSIF pH 5.0 media (Figure 6). Danazol dissolution from NaX-FAU in SGF showed a gradual increase over time reaching 70 % of the total drug content within 2 h (Figure 6A). At the same time-scale, crystalline danazol showed a burst dissolution (40 %) within 5 min followed by a plateau (50 %) until the end of the study. Similar dissolution profiles were also obtained for the pure crystalline drug and the drug-loaded zeolitic particles in FeSSIF (Figure 6B) with ca. 50 % of the total drug content dissolved at 2 h in both cases. However, it is evident that gradual release was attained from the zeolitic particles compared to the fast dissolution of the crystalline API, enabling control over the rate of drug release. Previously, it has been suggested that "poor sink conditions" can be introduced in an attempt to discriminate between formulations (mesoporous silica SBA-15) and crystalline APIs [49]. In this work, the dissolution of the total drug content in the release medium leads to a concentration that is about 20% of the drug's solubility. The higher drug dissolution from NaX-FAU in SGF can be attributed to the acidic nature of the medium, with previous studies [43 - 44], showing the NaX-FAU zeolites are prone to structural dissolution of their framework under acidic conditions. The dissolution mechanism of Faujasite

framework in acidic pH involves selective aluminum depletion and has been reported to solely depend on the framework compositions of Si/Al ratios between 1 and 3 [43],[45]. The dissolution profiles of danazol in FaSSIF conditions are illustrated in Figure 6C. Low dissolution rates were recorded for both crystalline danazol and NaX-FAU loaded danazol [46-47], while in both cases the amount of drug dissolved at 2 h was significantly lower compared to that dissolved in FeSSIF at the same time-sale. It has been previously reported [48] that the dissolution of danazol is dependent on the composition of the medium, where an increase to bile salt / phospholipid content results in enhanced dissolution rates, further corroborating the higher solubility of the lipophilic and non-ionized danazol in FeSSIF.

The results show that in media with high solubilization capacity [SGF 2% SLS, FeSSIF] drug release occurs in a gradual manner from the porous carrier, compared to the rapid dissolution of the pure API which is followed by a plateau indicating that drug diffusion out of the porous network of the NaX-FAU zeolite constitutes the rate-limiting step for drug release.

Furthermore, the HRTEM results obtained from the stability studies of the zeolitic particles in simulated intestinal fluids suggest that the dominant factor for danazol dissolution from the zeolitic particles is solely attributed to the textural properties and the encapsulation capacity (pore size) of the porous carriers in both media, since the zeolitic framework remains intact under both fasted and fed state conditions. In addition, drug encapsulation within the NaX-FAU zeolite enabled better control over danazol dissolution over time, as deducted from the gradual dissolution profiles observed for danazol from the NaX-FAU zeolite in all media.

The effect of danazol loading within the NaX-FAU zeolite on drug permeation across rat intestinal epithelium was determined using the everted gut sac method (Figure 7).

The permeated amount of danazol from the NaX-FAU zeolite formulation increased proportionally over time compared to the crystalline drug. A 2-fold higher relative permeability of danazol from the NaX-FAU formulation compared to crystalline danazol was recorded at 30 min (t-test, $p < 0.05$), whereas a significantly higher drug transport (twice higher compared to the control, t-test, $p < 0.05$) was observed at 120 min. The lower permeability of danazol in suspension form is attributed to its poor aqueous solubility in the mucosal compartment. The results indicate that the properties of the carrier acting as permeation enhancer, rather than its solubilization capacity can increase the transport of the API across intestinal epithelium. Previously, we have shown that the transepithelial resistance of Caco-2 monolayers was decreased in a reversible manner when incubated with the NaX-FAU zeolitic particles, indicating an increase in the intestinal barrier permeability [4, 44].

4. Conclusion

NaX-FAU zeolite was co-formulated with the poorly soluble drug danazol resulting in increased drug amorphization. No alterations in the solid-state properties of the drug were observed even after storage under accelerated stressing conditions for 6 months. The zeolitic formulation enabled a gradual and increasing drug dissolution in media simulating the GIT transit, while at the same time enhanced drug permeation across intestinal epithelium. Overall results demonstrate the potential of NaX-FAU as a promising platform for the oral delivery of the lipophilic and poorly water-soluble danazol.

Declaration of interest

The authors report no declaration of interest.

Funding sources

This research was supported by General Secretariat for Research and Technology - Research Program “Excellence II, 4766”.

The authors acknowledge financial support from the European Union under the Seventh Framework Program (Integrated Infrastructure Initiative No. 262348 European Soft Matter Infrastructure, ESMI).

References

[1] Y. Wang, Q. Zhao, Y. Hu, L. Sun, L. Bai, T. Jiang, S. Wang, Ordered nanoporous silica as carriers for improved delivery of water insoluble drugs: a comparative study between three dimensional and two dimensional macroporous silica, Int. J. Nanomedicine. (2013) 4015. doi:10.2147/IJN.S52605.

[2] M. Filippousi, S. Turner, K. Leus, P.I. Siafaka, E.D. Tseligka, M. Vandichel, S.G. Nanaki, I.S. Vizirianakis, D.N. Bikiaris, P. Van Der Voort, G. Van Tendeloo, Biocompatible Zr-based nanoscale MOFs coated with modified poly(ε-caprolactone) as anticancer drug carriers, Int. J. Pharm. 509 (2016) 208-218. doi:10.1016/j.ijpharm.2016.05.048.

[3] M. Filippousi, P.I. Siafaka, E.P. Amanatiadou, S.G. Nanaki, M. Nerantzaki,

D.N. Bikiaris, I.S.Vizirianakis, G.Van Tendeloo, Modified chitosan coated mesoporous strontium hydroxyapatite nanorods as drug carriers, J. Mater. Chem. B. 3 (2015) 5991- 6000. doi:10.1039/C5TB00827A.

[4] M. Spanakis, N. Bouropoulos, D. Theodoropoulos, L. Sygellou, S. Ewart, A.M. Moschovi, A. Siokou, I. Niopas, K. Kachrimanis, V. Nikolakis, P.A. Cox, I.S. Vizirianakis, D.G. Fatouros, Controlled release of 5-fluorouracil from microporous zeolites, Nanomedicine Nanotechnology, Biol. Med. 10 (2014) 197-205. doi:10.1016/j.nano.2013.06.016.

[5] C. Karavasili, E.P. Amanatiadou, L. Sygellou, D.K. Giasafaki, T.A. Steriotis, G.C. Charalambopoulou, I.S. Vizirianakis, D.G. Fatouros, Development of new drug delivery system based on ordered mesoporous carbons: characterisation and cytocompatibility studies, J. Mater. Chem. B. 1 (2013) 3167. doi:10.1039/c3tb20304b.

[6] G.K. Eleftheriadis, M. Filippousi, V. Tsachouridou, M.-A. Darda, L. Sygellou, I. Kontopoulou, N. Bouropoulos, T. Steriotis, G. Charalambopoulou, I.S. Vizirianakis, G. Van Tendeloo, D.G. Fatouros, Evaluation of mesoporous carbon aerogels as carriers of the non-steroidal anti-inflammatory drug ibuprofen, Int. J. Pharm. 515 (2016) 262-270. doi:10.1016/j.ijpharm.2016.10.008.

[7] R. Amorim, N. Vilaça, O. Martinho, R.M. Reis, M. Sardo, J. Rocha, A.M. Fonseca, F. Baltazar, I.C. Neves, Zeolite structures loading with an anticancer compound as drug delivery systems, J. Phys. Chem. C. 116 (2012) 25642-25650. doi:10.1021/jp3093868.

[8] A. Datt, E.A. Burns, N.A. Dhuna, S.C. Larsen, Loading and release of 5-fluorouracil from HY zeolites with varying SiO_2/Al_2O_3 ratios, Microporous

Mesoporous Mater. 167 (2013) 182-187. doi:10.1016/j.micromeso.2012.09.011.

[9] N. Paradee, A. Sirivat, Encapsulation of folic acid in zeolite Y for controlled release via electric field, Mol. Pharm. 13 (2016) 155-162. doi:10.1021/acs.molpharmaceut.5b00592.

[10] H. Lülf, A. Bertucci, D. Septiadi, R. Corradini, L. De Cola, Multifunctional inorganic nanocontainers for DNA and drug delivery into living cells, Chem. - A Eur. J. 20 (2014) 10900-10904. doi:10.1002/chem.201403232.

[11] M.G. Rimoli, M.R. Rabaioli, D. Melisi, A. Curcio, S. Mondello, R. Mirabelli, E. Abignente, Synthetic zeolites as a new tool for drug delivery, J. Biomed. Mater. Res. Part A. 87A (2008) 156-164. doi:10.1002/jbm.a.31763.

[12] A. Datt, D.Fields, S.C. Larsen. An experimental and computational study of the loading and release of aspirin from zeolite HY, J. Phys. Chem C. C 116 (2012), 21382-21390 doi: 10.1021/jp3067266

[13] A.Datt, E.A. Burns, N.A. Dhuna, S.C. Larsen. Loading and release of 5-fluorouracil from HY zeolites with varying SiO_2/Al_2O_3 ratios, Microporous Mesoporous Mater. 167 (2013) 182-187 doi:10.1016/j.micromeso.2012.09.011

[14] P. Horcajada, C. Márquez-Alvarez, A. Rámila, J. Pérez-Pariente, M. Vallet-Regí. Controlled release of ibuprofen from dealuminated faujasites, Solid State Sci. 8. (2006), 1459-1465 doi:10.1016/j.solidstatesciences.2006.07.016

[15] M. Khatamian, A. Yavari, A. Akbarzadeh, E.Alizadeh. Synthesis and characterization of MFI-type borosilicate zeolites and evaluation of their efficiency as drug delivery systems, Mater Sci Eng C Mater Biol Appl. 78 (2017) 1212-1221 doi: 10.1016/j.msec.2017.03.008

[16] F. Yang, X. Wen, Q.F. Ke, X.T. Xie, Y.P. Guo. pH-responsive mesoporous

ZSM-5 zeolites/chitosan core-shell nanodisks loaded with doxorubicin against osteosarcoma, Mater Sci Eng C Mater Biol Appl. 85 (2018) 85142-153 doi: 10.1016/j.msec.2017.12.024.

[17] C. Serri, B. de Gennaro, V. Quagliariello, R,V. Iaffaioli, G. De Rosa, L. Catalanotti M. Biondi, L. Mayol. Surface modified zeolite-based granulates for the sustained release of diclofenac sodium, Eur J Pharm Sci. (99) 2017 202-208 doi: 10.1016/j.ejps.2016.12.019

[18] B. de Gennaro, L. Catalanotti, P. Cappelletti, A. Langella, M. Mercurio, C. Serri, M. Biondi, L. Mayol. Surface modified natural zeolite as a carrier for sustained diclofenac release: A preliminary feasibility study, Colloids Surf B Biointerfaces. 130 (2015) 101-109 doi: 10.1016/j.colsurfb.2015.03.052

[19] A. Bertucci, H. Lülf, D. Septiadi, A. Manicardi, R. Corradini, L. De Cola. Intracellular delivery of peptide nucleic acid and organic molecules using zeolite-L nanocrystals, Adv Healthc Mater. (3) 2014 1812-1827 doi: 10.1002/adhm.201400116

[20] D. Krajišnik, R. Stepanović-Petrović, M. Tomić, A. Micov, S. Ibrić, J.Milić. Application of artificial neural networks in prediction of diclofenac sodium release from drug-modified zeolites physical mixtures and antiedematous activity assessment, J Pharm Sci. 103 (2014) 1085-1094 doi: 10.1002/jps.23869

[21] S. Grund, T. Doussineau, D. Fischer, G.J.Mohr. Mitoxantrone-loaded zeolite beta nanoparticles: preparation, physico-chemical characterization and biological evaluation, J Colloid Interface Sci. (365) 2012 33-40. doi: 10.1016/j.jcis.2011.09.003

[22] Y.-P. Guo, T. Long, Z.-F. Song, Z.-A. Zhu, Hydrothermal fabrication of ZSM-5 zeolites: Biocompatibility, drug delivery property, and bactericidal property,

J. Biomed. Mater. Res. Part B Appl. Biomater. 102 (2014) 583-591. doi:10.1002/jbm.b.33037.

[23] N. Vilaça, R. Amorim, A.F. Machado, P. Parpot, M.F.R. Pereira, M. Sardo, J. Rocha, A.M. Fonseca, I.C. Neves, F. Baltazar, Potentiation of 5-fluorouracil encapsulated in zeolites as drug delivery systems for in vitro models of colorectal carcinoma, Colloids Surfaces B Biointerfaces. 112 (2013) 237-244. doi:10.1016/j.colsurfb.2013.07.042.

[24] C. Karavasili, L. Kokove, I. Kontopoulou, G.K. Eleftheriadis, N. Bouropoulos, D.G. Fatouros, Dissolution enhancement of the poorly soluble drug nifedipine by co-spray drying with microporous zeolite beta, J. Drug Deliv. Sci. Technol. 35 (2016) 91-97. doi:10.1016/j.jddst.2016.06.004.

[25] D.G. Fatouros, D. Douroumis, V. Nikolakis, S. Ntais, A.M. Moschovi, V. Trivedi, B. Khima, M. Roldo, H. Nazar, P.A. Cox, In vitro and in silico investigations of drug delivery via zeolite BEA, J. Mater. Chem. 21 (2011) 7789. doi:10.1039/c1jm10204d.

[26] A. Dyer, S. Morgan, P. Wells, C. Williams, The use of zeolites as slow release anthelmintic carriers. J. Helminthol. 74 (2000) 137-141. http://www.ncbi.nlm.nih.gov/pubmed/10881284.

[27] C.S.Cundy, P.A.Cox. The hydrothermal synthesis of zeolites: history and development from the earliest days to the present time, Chem Rev. (103) 2003 663-702 doi:10.1021/cr020060i

[28] S.L.Suib. A review of recent developments of mesoporous materials, Chem Rec. (12) 2017 1169-1183 doi: 10.1002/tcr.201700025

[29] L. Bacakova, M. Vandrovcova, I. Kopova, I.Jirka. Applications of zeolites in biotechnology and medicine - a review, Biomater Sci. (6) 2018 974-989 doi:

10.1039/c8bm00028j

[30] C.Laurino, B.Palmieri. Zeolite : "The magic stone"; main nutritional, enviromental, experimental and clinical fields of application, Nutr Hosp. 32 (2015) 573-581 doi: 10.3305/nh.2015.32.2.8914

[31] S.Ivkovic, U.Deutsch, A.Silberbach, E.Walraph, M.Mannel. Dietary supplementation with the tribomechanically activated zeolite clinoptilolite in immunodeficiency: effects on the immune system, Advances in therapy 21 (2004) 135-147

[32] W.Potgieter, C.S.Samuels, J.R.Snyman. Potentiated clinoptilolite: artificially enhanced aluminosilicate reduces symptoms associated with endoscopically negative gastroesophageal reflux disease and nonsteroidal anti-inflammatory drug induced gastritis, Clin Exp Gastroenterol (7) 2014 215-220 doi: 10.2147/CEG.S51222

[33] C. Markopoulos, F. Thoenen, D. Preisig, M. Symillides, M. Vertzoni, N. Parrott, C. Reppas, G. Imanidis, Biorelevant media for transport experiments in the Caco-2 model to evaluate drug absorption in the fasted and the fed state and their usefulness, Eur. J. Pharm. Biopharm. 86 (2014) 438-448. doi:10.1016/j.ejpb.2013.10.017.

[34] S.L. Childs, P. Kandi, S.R. Lingireddy, Formulation of a danazol cocrystal with controlled supersaturation plays an essential role in improving bioavailability, Mol. Pharm. 10 (2013) 3112-3127. doi:10.1021/mp400176y.

[35] M. Vertzoni, N. Fotaki, E. Nicolaides, C. Reppas, E. Kostewicz, E. Stippler, C. Leuner, J. Dressman, Dissolution media simulating the intralumenal composition of the small intestine: physiological issues and practical aspects, J. Pharm. Pharmacol. 56 (2004) 453-462. doi:10.1211/0022357022935.

[36] E. Sayed, C. Karavasili, K. Ruparelia, R. Haj-Ahmad, G. Charalambopoulou, T. Steriotis, D. Giasafaki, P. Cox, N. Singh, L.-P.N. Giassafaki, A. Mpenekou, C.K. Markopoulou, I.S. Vizirianakis, M.-W. Chang, D.G. Fatouros, Z. Ahmad, Electrosprayed mesoporous particles for improved aqueous solubility of a poorly water soluble anticancer agent: in vitro and ex vivo evaluation, J. Control. Release. 278 (2018) 142-155. doi:10.1016/j.jconrel.2018.03.031.

[37] J. Guo, Q. Ping, G. Jiang, J. Dong, S. Qi, L. Feng, Z. Li, C. Li, Transport of leuprolide across rat intestine, rabbit intestine and Caco-2 cell monolayer, Int. J. Pharm. 278 (2004) 415-422. doi:10.1016/j.ijpharm.2004.03.031.

[38] G.P. Lambert, C. V. Gisolfi, D.J. Berg, P.L. Moseley, L.W. Oberley, K.C. Kregel, Selected Contribution: Hyperthermia-induced intestinal permeability and the role of oxidative and nitrosative stress, J. Appl. Physiol. 92 (2002) 1750-1761. doi:10.1152/japplphysiol.00787.2001.

[39] C.Karavasili, M.Spanakis, D.Papagiannopoulou, I.S.Vizirianakis, D.G. Fatouros, S. Koutsopoulos, Bioactive self-assembling lipid-like peptides as permeation enhancers for oral drug delivery, J. Pharm. Sci. 104 (2015) 2304-2311. doi:10.1002/jps.24484.

[40] S.I. Farag Badawy, M.M. Ghorab, C.M. Adeyeye, Characterization and bioavailability of danazol-hydroxypropyl β-cyclodextrin coprecipitates, Int. J. Pharm. 128 (1996) 45-54. doi:10.1016/0378-5173(95)04214-8.

[41] J.Hu, K.P.Johnston, R.O.Williams 3rd. Stable amorphous danazol nanostructured powders with rapid dissolution rates produced by spray freezing into liquid drug, Dev Ind Pharm. (30) 2004 695-704 doi: 10.1081/DDC-120039212

[42] M.M.J. Treacy, Collection of simulated XRD powder patterns for zeolites Editors :, (2001). doi:http://dx.doi.org/10.1016/S0166-9834(00)81382-2.

[43] R.L. Hartman, H.S. Fogler, Understanding the dissolution of zeolites, Langmuir. 23 (2007) 5477-5484. doi:10.1021/la063699g.

[44] C. Karavasili, E.P. Amanatiadou, E. Kontogiannidou, G.K. Eleftheriadis, N. Bouropoulos, E. Pavlidou, I. Kontopoulou, I.S. Vizirianakis, D.G. Fatouros, Comparison of different zeolite framework types as carriers for the oral delivery of the poorly soluble drug indomethacin, Int. J. Pharm. 528 (2017) 76-87. doi:10.1016/j.ijpharm.2017.05.061.

[45] R.L. Hartman, H.S. Fogler, Reaction kinetics and mechanisms of zeolite dissolution in hydrochloric acid, Ind. Eng. Chem. Res. 44 (2005) 7738-7745. doi:10.1021/ie0504349.

[46] J.H. Fagerberg, O. Tsinman, N. Sun, K. Tsinman, A. Avdeef, C.A.S. Bergström, Dissolution rate and apparent solubility of poorly soluble drugs in biorelevant dissolution media, Mol. Pharm. 7 (2010) 1419-1430. doi:10.1021/mp100049m.

[47] V.H. Sunesen, B.L. Pedersen, H.G. Kristensen, A. Müllertz, In vivo in vitro correlations for a poorly soluble drug, danazol, using the flow-through dissolution method with biorelevant dissolution media, Eur. J. Pharm. Sci. 24 (2005) 305-313. doi:10.1016/j.ejps.2004.11.007.

[48] E. Galia, E. Nicolaides, D. Hörter, R. Löbenberg, C. Reppas, J.B. Dressman, Evaluation of various dissolution media for predicting in vivo performance of class I and II drugs, Pharm. Res. 15 (1998) 698-705. http://www.ncbi.nlm.nih.gov/pubmed/9619777.

[49] M. Van Speybroeck, V. Barillaro, T.D. Thi, R. Mellaerts, J. Martens, J. Van Humbeeck, J. Vermant, P. Annaert, G. Van den Mooter, P. Augustijns. Ordered mesoporous silica material SBA-15: a broad-spectrum formulation platform for

poorly soluble drugs J Pharm Sci. 98 (2009) 2648 - 2658 doi: 10.1002/jps.21638

Table 1: Drug content (%) as calculated by UV analysis and TGA and ζ-potential of pristine and drug-loaded NaX-FAU zeolitic particles.

Carrier	Drug content (%) (TGA)*	Drug content (%) (UV)*	ζ-potential (mV)#
NaX (E)	-	-	-55.1 ± 2.4
NaX (L)	31.1 ± 0.4	30.9 ± 0.9	-32.7 ± 1.4

E: empty carrier, L: Danazol loaded, * (n=2), # (n=3)

570

571 **Table 2**: Textural properties of the empty and drug loaded NaX-FAU particles.

Carrier	BET surface area (m^2/g)[a]	Micropore area (m^2/g)	External surface area (m^2/g)	Total pore volume (cm^3/g)[b]
NaX (E)	715.24	693.55	21.69	0.28
NaX (L)	4.99	4.05	0.94	0.01

572 [a] SBET (m^2/g): BET surface area. [b] Vt (cm^3/g): total pore volume calculated as the amount of nitrogen

573 adsorbed at a relative pressure of 0.995.

574

575

576

577

578

579

580

581

582 **FIGURE LEGENDS**

583 **FIGURE 1**: **(A)** TGA, (**B**) DSC and (**C**) XRD analysis of NaX-FAU zeolite,
584 crystalline danazol and the zeolitic formulation.

585

586 **FIGURE 2**: **(A)** N_2 adsorption-desorption isotherms and (**B**) pore size distribution of
587 the zeolite and the danazol-loaded zeolite formulation.

588

589 **FIGURE 3**: **(A)** Low and (**B**) high magnification TEM images of pristine NaX-FAU
590 zeolitic particles. The SAED and FFT patterns are given as inset in **(A)** and **(B)**,
591 respectively.

592

593 **FIGURE 4**: **(A)** DSC thermograms and **(B)** X-ray diffractograms of danazol-loaded
594 zeolite formulation after 6 months testing at accelerated storage conditions.

595

596 **FIGURE 5**: Low and high magnification TEM images of empty and drug loaded
597 NaX-FAU particles in **(A-B)** FaSSIF and **(C-F)** FeSSIF media. No effect on the
598 morphology or the structure of the zeolitic particles could be identified upon exposure
599 to these media.

600

601 **FIGURE 6**: *In vitro* dissolution profiles of crystalline danazol and drug-loaded NaX-
602 FAU in (**A)** simulated gastric fluid (SGF) pH 1.2 in the presence of 2 % SLS, (**B)** fed
603 state simulated intestinal fluid (FeSSIF) pH 5.0 and (**C)** fasted state simulated
604 intestinal fluid (FaSSIF) pH 6.5 at 37 ^{o}C.

605

FIGURE 7: Relative permeability (μg/cm^2) of crystalline danazol and danazol-loaded NaX-FAU formulation at 30 min and 120 min using the everted sac method. In each box chart, the bottom (×) shows the minimum value and marks the 0th percentile. The bottom of the box marks the 25th percentile and the top of the box marks the 75th percentile. The square symbol (□) in the box marks the mean value. The top (×) shows the maximum value and 100th percentile. Results are the mean values of n = 4 - 8.

FIGURE 1

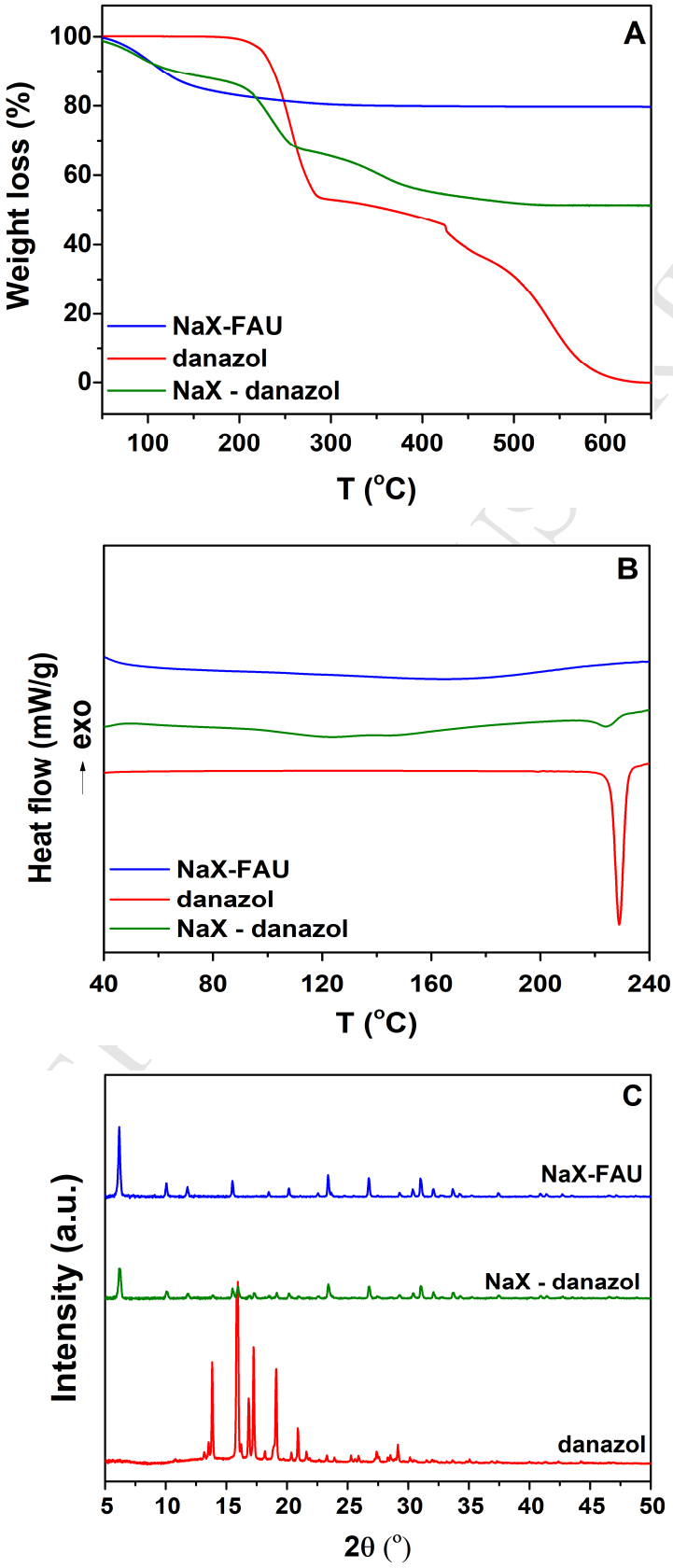
A
Weight loss (%)
100
80
60
40
20
0
NaX-FAU
danazol
NaX - danazol
100
200
300
400
500
600
T (°C)
B
Heat flow (mW/g)
exo
NaX-FAU
danazol
NaX - danazol
40
80
120
160
200
240
T (°C)
C
Intensity (a.u.)
NaX-FAU
NaX - danazol
danazol
5
10
15
20
25
30
35
40
45
50
2θ (°)

FIGURE 2

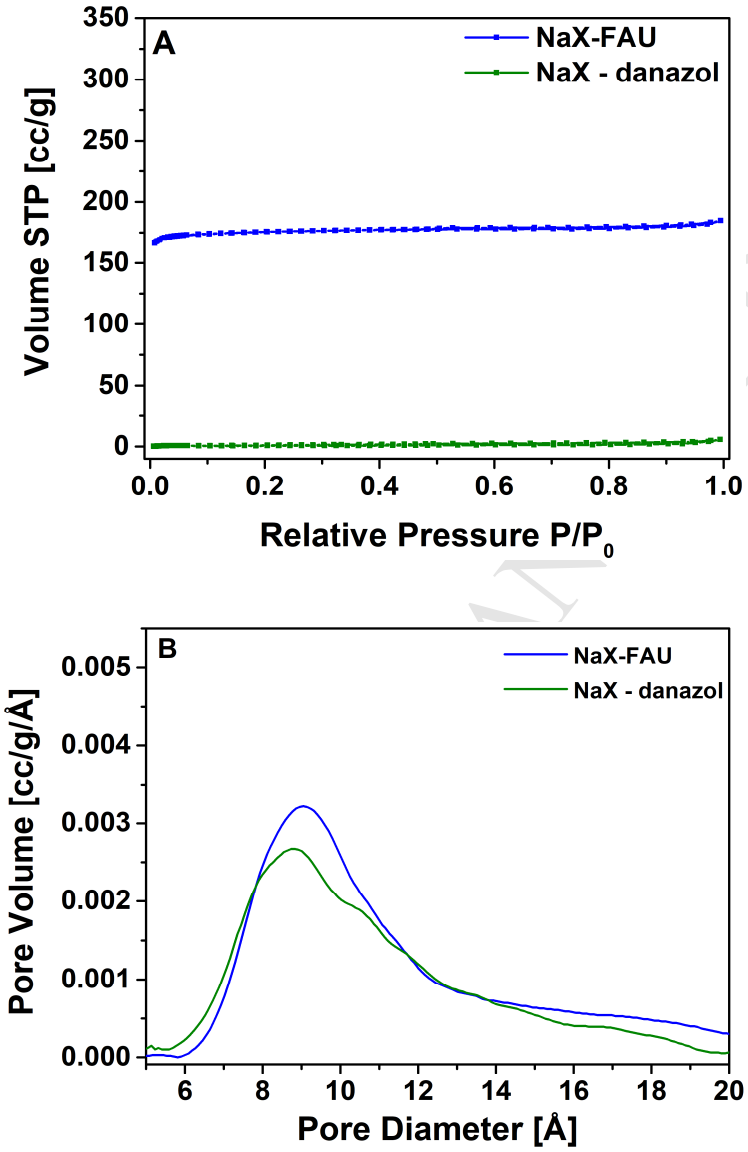
A
NaX-FAU
NaX - danazol
Volume STP [cc/g]
Relative Pressure P/P0
B
NaX-FAU
NaX - danazol
Pore Volume [cc/g/Å]
Pore Diameter [Å]

FIGURE 3

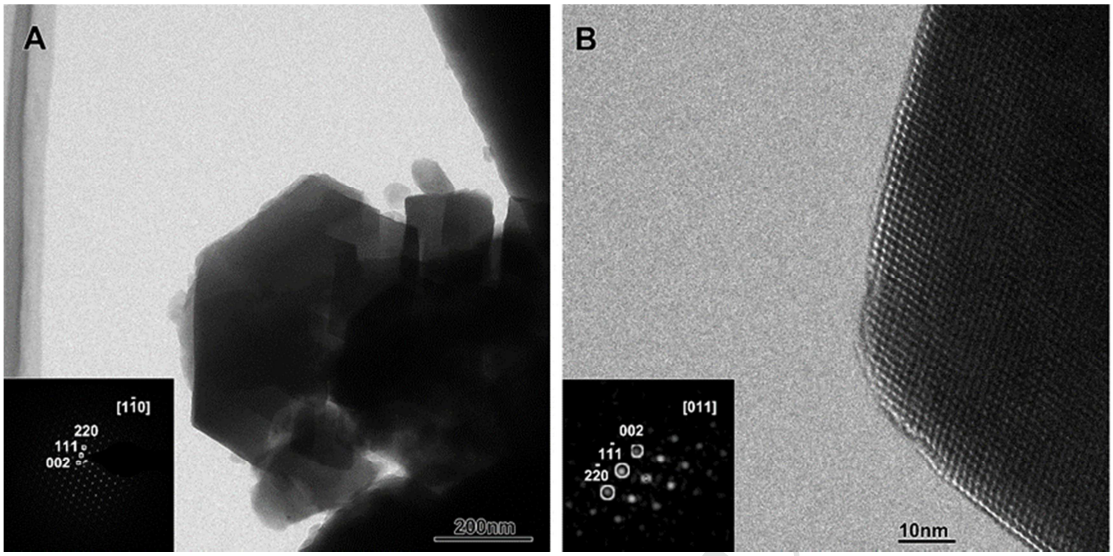

FIGURE 4

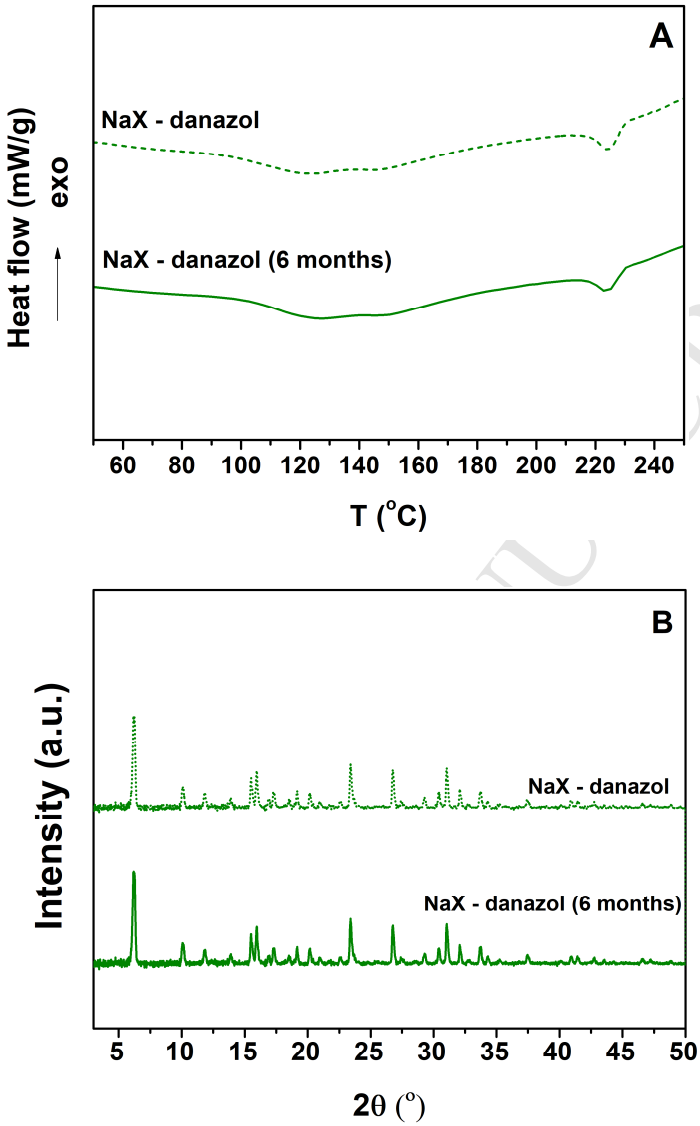
A
NaX - danazol
NaX - danazol (6 months)
Heat flow (mW/g)
exo
60 80 100 120 140 160 180 200 220 240
T (°C)
B
NaX - danazol
NaX - danazol (6 months)
Intensity (a.u.)
5 10 15 20 25 30 35 40 45 50
2θ (°)

719 **FIGURE 5**

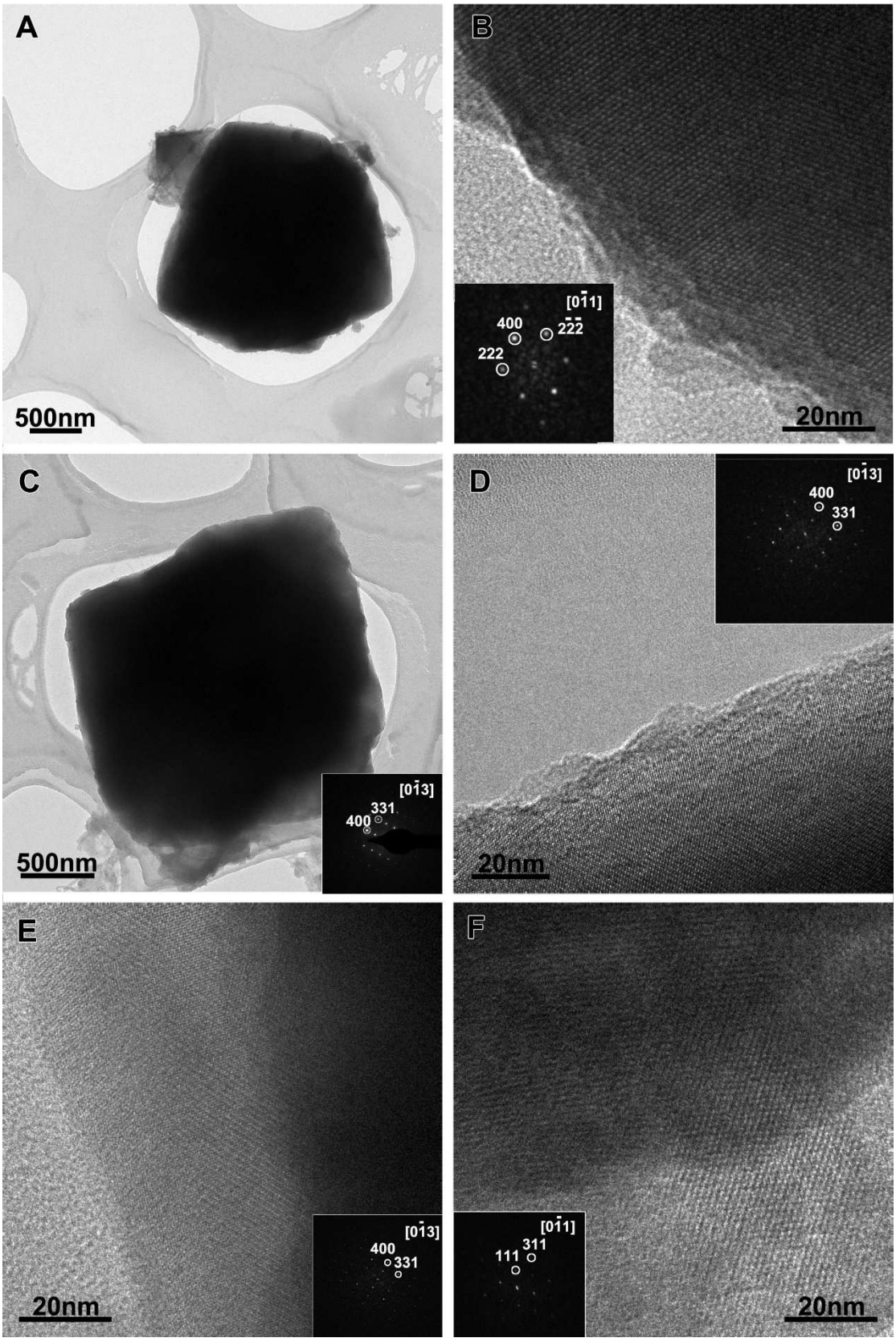

720

721

FIGURE 6

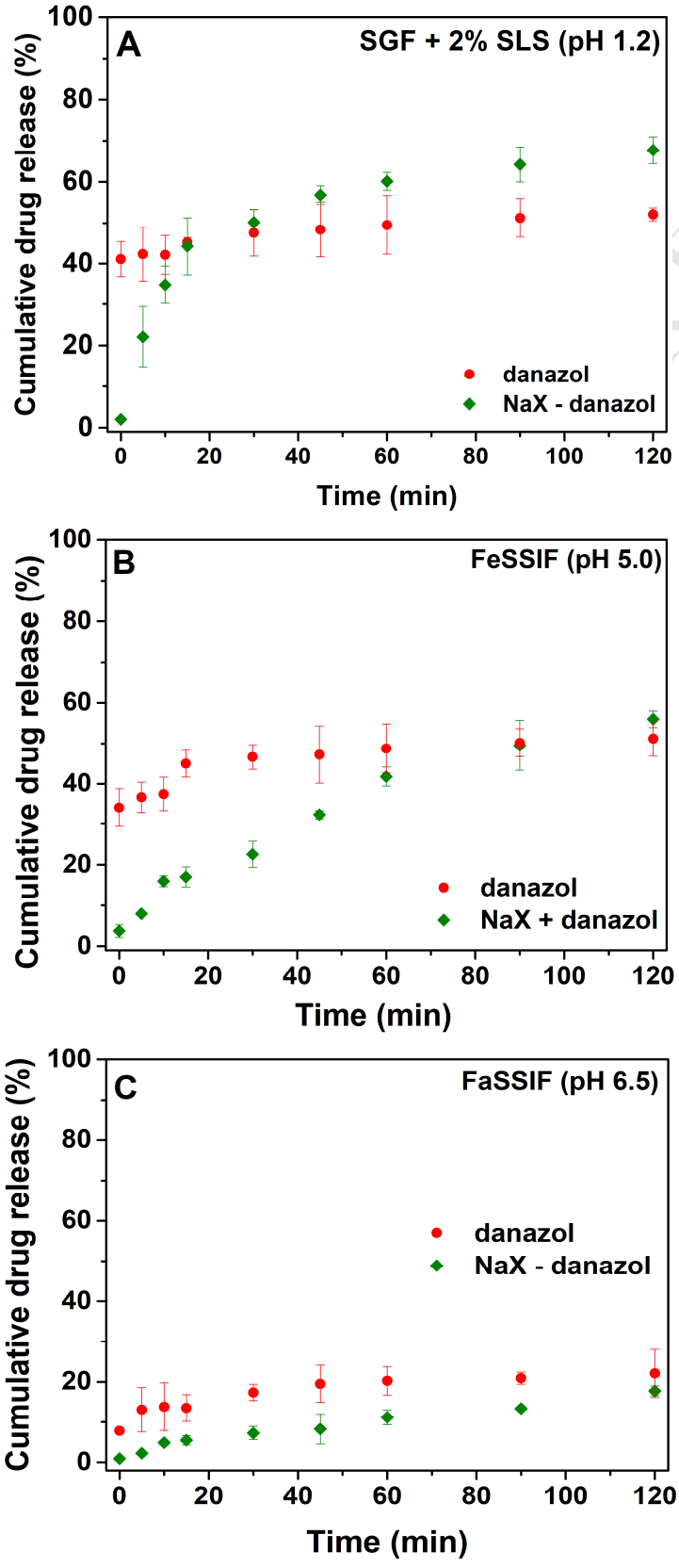
A
SGF + 2% SLS (pH 1.2)
Cumulative drug release (%)
Time (min)
danazol
NaX - danazol
B
FeSSIF (pH 5.0)
Cumulative drug release (%)
Time (min)
danazol
NaX + danazol
C
FaSSIF (pH 6.5)
Cumulative drug release (%)
Time (min)
danazol
NaX - danazol

747 **FIGURE 7**

748

749